MgZnO *p–n* heterostructure light-emitting devices

Ji-Shan Liu,[1,2] Chong-Xin Shan,[1,*] Bing-Hui Li,[1] Zhen-Zhong Zhang,[1] Ke-Wei Liu,[1] and De-Zhen Shen[1]

[1]*State Key Laboratory of Luminescence and Applications, Changchun Institute of Optics, Fine Mechanics and Physics, Chinese Academy of Sciences, No. 3888 Dongnanhu Road, Changchun 130033, China*

[2]*University of Chinese Academy of Sciences, Beijing 100049, China*

**Corresponding author: shancx@ciomp.ac.cn*

Received March 4, 2013; revised May 9, 2013; accepted May 13, 2013; posted May 15, 2013 (Doc. ID 186324); published June 11, 2013

MgZnO heterostructure light-emitting devices (LEDs) have been fabricated from p-$Mg_{0.35}Zn_{0.65}O/n$-$Mg_{0.20}Zn_{0.80}O$ structures, and the p-type $Mg_{0.35}Zn_{0.65}O$ film was realized using a lithium–nitrogen codoping method. Obvious ultraviolet emission peaked at around 355 nm dominates the electroluminescence (EL) spectra of the device at room temperature, which comes from the near-band-edge emission of the n-type $Mg_{0.20}Zn_{0.80}O$ film. This is the first report on MgZnO heterostructured LEDs and the shortest EL emission ever reported in ZnO-based p-n junction LEDs to the best of our knowledge. © 2013 Optical Society of America

OCIS codes: (310.6845) Thin film devices and applications; (260.3800) Luminescence; (260.7190) Ultraviolet; (250.0250) Optoelectronics.

http://dx.doi.org/10.1364/OL.38.002113

Ultraviolet (UV) semiconductor photonic devices such as light-emitting devices (LEDs) and laser diodes have attracted considerable attention in recent years for their versatile applications such as efficient lighting, sterilization, water purification, medical diagnostics, and so forth [1,2]. Because of its wide direct bandgap and large exciton binding energy, ZnO has been considered as one of the promising candidates for UV LEDs [3–5]. Some reports have demonstrated ZnO-based p-n junction LEDs recently [6–8]. Nevertheless, considering that efficient p-type doping of ZnO is still a huge challenge, many researchers have devotes effort to ZnO-based heterojunction LEDs by combining n-ZnO with other p-type materials, such as p-GaN [9] and p-SiC [10], etc. It is accepted that due to the large difference in the physical properties and chemical bonding states of the two materials, surface defects will usually form at the interface, which will degrade the performance of the heterojunction LEDs drastically. Heterostructures constituted by alloyed semiconductors with different composition can ensure efficient carrier injection and confinement, thus they are effective in improving the performance of LEDs. Nevertheless, the reports on ZnO-based heterostructured LEDs are still very limited [11–13]. Another interesting character of ZnO lies in its tunable bandgap when alloyed with MgO, which implies that ZnO-based materials may find applications in shorter-wavelength LEDs [14–16]. However, the emissions of the ZnO-based LEDs reported so far are all located in the region longer than 375 nm, which corresponds to the near-band-edge emission of ZnO, while no report on shorter-wavelength ZnO-based LEDs can be found up to now.

In a previous study, reproducible p-type ZnO films have been realized, and reliable ZnO-based p-n junction LEDs that can operate continuously for several hours have been fabricated [17,18]. In this Letter, by employing a lithium nitrogen (Li,N) codoping method, p-type $Mg_{0.35}Zn_{0.65}O$ films have been prepared, and p-$Mg_{0.35}Zn_{0.65}O/n$-$Mg_{0.20}Zn_{0.80}O$ heterostructured LEDs have been fabricated. Dominant UV emission peaked at around 355 nm has been observed from the heterostructures.

The MgZnO films investigated in this study were grown on a-plane sapphire in a VG V80H plasma-assisted molecular beam epitaxy technique. First, a 400 nm n-type $Mg_{0.20}Zn_{0.80}O$ film was grown onto the sapphire substrate; the detailed growth conditions can be found elsewhere [19]. After that, Li,N-codoped p-type $Mg_{0.35}Zn_{0.65}O$ film was deposited onto the n-type $Mg_{0.20}Zn_{0.80}O$ film to form the heterostructure. For the p-type doping of the $Mg_{0.35}Zn_{0.65}O$, elemental Zn, Li, and Mg contained in individual Knudsen cells were employed as precursors, and atomic oxygen and nitrogen generated from NO gas (6N) via a plasma cell was used as the O and N source. The growth chamber pressure and substrate temperature were set at 1.5×10^{-5} mbar and 700°C during the growth, respectively. Metallic In and Ni/Au layers were deposited onto the n-$Mg_{0.20}Zn_{0.80}O$ and $Mg_{0.35}Zn_{0.65}O$:(Li, N) layers acting as ohmic contacts by a thermal evaporation method.

The electrical properties of the films were measured by a Hall system. The composition of the MgZnO layers was determined using energy dispersive x-ray spectroscopy (EDS). An AXIS Ultra^{DLD} x-ray photoelectron spectroscope (XPS) has been employed to measure the doping concentration of the dopants. The photoluminescence (PL) spectra of the n-$Mg_{0.20}Zn_{0.80}O$ films were recorded using the 325 nm line of an He–Cd laser as the excitation source, and those of the $Mg_{0.35}Zn_{0.65}O$ layer were carried out under the excitation of the 266 nm line of a YAG:Nd laser. EL measurements of the heterostructured LEDs were carried out in a Hitachi F4500 spectrometer under the drive of a continuous-current power source.

The electron concentration and Hall mobility of the n-type $Mg_{0.20}Zn_{0.80}O$ film are $2.7 \times 10^{19}\ cm^{-3}$ and $23\ cm^2/Vs$, respectively. Such a low resistivity is favorable for constructing light-emitting structures. The Li and N concentration in the $Mg_{0.35}Zn_{0.65}O$:(Li, N) film determined by XPS is around 1.84% and 0.43%, respectively. Hall measurement on the $Mg_{0.35}Zn_{0.65}O$:(Li, N) film shows p-type conduction with a hole concentration of about $1.6 \times 10^{16}\ cm^{-3}$ and a mobility of $1.3\ cm^2/Vs$. The formation mechanism of Li,N-codoped p-type ZnO-based films have been investigated before [17,20], and

 © 2013 Optical Society of America

it has been speculated that Li substituted Zn(Mg) ($Li_{Zn(Mg)}$) acts as acceptors, while the incorporated N may passivate the interstitial Li donors to reduce the possible compensation to $Li_{Zn(Mg)}$ acceptors.

The structural properties of the MgZnO films characterized by x-ray diffractometer (XRD) are shown in Fig. 1. Only one strong peak at 34.61° and 34.69° can be observed from the patterns of the n-type and p-type layers, respectively, which reveals that both the films are crystallized in a hexagonal wurtzite structure with (0002) preferred orientation. The larger angle of the p-type layer than the n-type layer indicates higher Mg composition of the p-type layer, which is consistent with the EDS data.

To assess the optical properties of the MgZnO layers, absorption and PL spectra of these layers have been measured, the results of which are shown in Fig. 2. One can see from Fig. 2(a) that the n-$Mg_{0.20}Zn_{0.80}O$ film shows a strong absorption in the UV region with a sharp absorption edge at around 344 nm. From the absorption spectrum, a bandgap of around 3.60 eV can be derived for the n-$Mg_{0.20}Zn_{0.80}O$ film by employing the $\alpha^2 \propto (h\nu - E_g)$ expression, where α is the absorption coefficient and $h\nu$ is the photon energy. The PL spectrum of the n-$Mg_{0.20}Zn_{0.80}O$ layer displays a strong Gaussian lineshape peaked at around 349 nm, which can be attributed to the near-band-edge emission of the $Mg_{0.20}Zn_{0.80}O$ film. The absorption edge of the $Mg_{0.35}Zn_{0.65}O$:(Li, N) layer is located at around 330 nm, as shown in Fig. 2(b), from which a bandgap of around 3.75 eV can be derived. The PL spectrum of the $Mg_{0.35}Zn_{0.65}O$:(Li, N) shows a broad emission peak at around 336 nm. The broadening of the PL spectrum may come from the composition fluctuation in this layer.

The current–voltage (I–V) curve of the heterostructure is illustrated in Fig. 3. Obvious rectifying behaviors are observed in the I–V curve. The turn-on voltage of the structure is about 6.0 V. Note that the sheet resistance of the structure deduced from the I–V curve is around 252Ω. Shown in the inset of Fig. 3 is the I–V curve of the Ni–Au electrode on the p-type $Mg_{0.35}Zn_{0.65}O$:(Li, N) layer and the In electrode on the n-type $Mg_{0.20}Zn_{0.80}O$ layer. The linear I–V curves reveal that ohmic contacts have been obtained in both cases. The ohmic behaviors of the metal contacts exclude the possibility of the formation of any Schottky junction in the device, confirming the rectification behaviors arise from the heterostructure.

The room-temperature EL spectra of the p-$Mg_{0.35}Zn_{0.65}O$:(Li, N)/n-$Mg_{0.20}Zn_{0.80}O$ heterostructure at various injection currents are shown in Fig. 4. All the spectra are dominated by an emission band peaked at around 355 nm, which can be attributed to the near-band-edge emission of the n-$Mg_{0.20}Zn_{0.80}O$ as its position

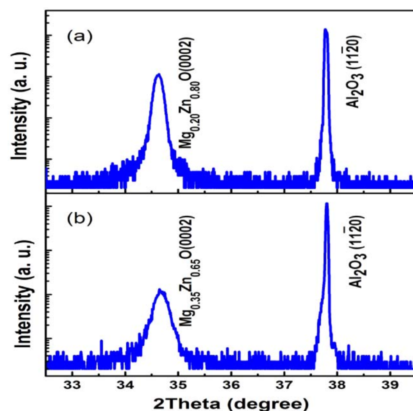

Fig. 1. XRD pattern of the (a) n-type $Mg_{0.20}Zn_{0.80}O$ and (b) p-type $Mg_{0.35}Zn_{0.65}O$:(Li, N) layers grown on a-plane sapphire.

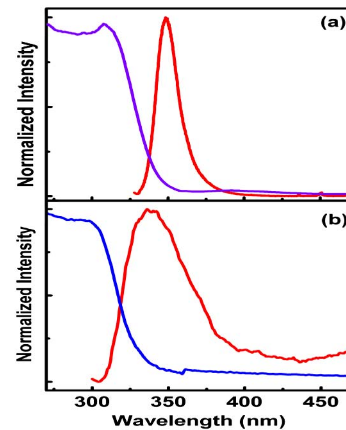

Fig. 2. Normalized absorption and PL spectra of the (a) n-type $Mg_{0.20}Zn_{0.80}O$ layer and (b) p-type $Mg_{0.35}Zn_{0.65}O$:(Li, N) layer.

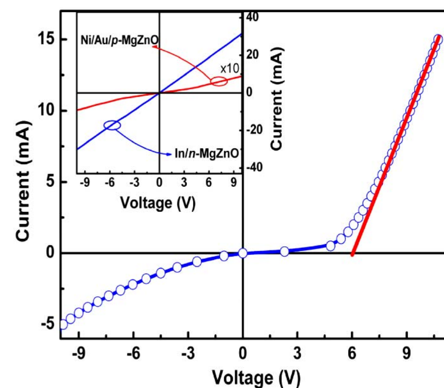

Fig. 3. I–V characteristics of the p-$Mg_{0.35}Zn_{0.65}O$:(Li, N)/n-$Mg_{0.20}Zn_{0.80}O$ heterostructure; the inset shows the I–V curves of the Ni/Au contact on the p-type layer and the In contact on the n-type layer.

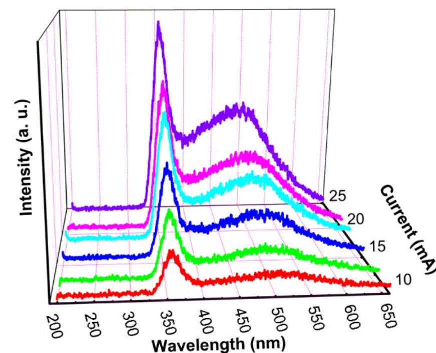

Fig. 4. Room-temperature EL spectra of the p-$Mg_{0.35}Zn_{0.65}O$:(Li, N)/n-$Mg_{0.20}Zn_{0.80}O$ heterostructure at different injection currents.

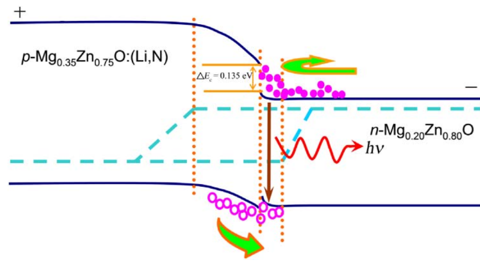

Fig. 5. Schematic bandgap diagram of the p-$Mg_{0.35}Zn_{0.65}O$:(Li, N)/n-$Mg_{0.20}Zn_{0.80}O$ heterostructure under forward bias.

is very close to the PL peak of this layer (349 nm). Additionally, a broad emission at around 500 nm can also be observed from the EL spectra, which has been frequently observed in ZnO-based LEDs [15,21], and may come from the deep-level-related emission in ZnO-based materials. We note that the defects-related emission does not appear in the PL, while it does in the EL spectra of the heterostructure. The reason for the discrepancy may be as follows: In EL the recombination of electrons and holes occur at the p-$Mg_{0.35}Zn_{0.65}O$:(Li, N)/n-$Mg_{0.20}Zn_{0.80}O$ interface, while the interface usually has a relatively high defect density. Consequently, deep-level-related emission is observed in the EL spectra. Meanwhile, PL emission comes from the n-type or p-type layer but not from the interface, where the defect density inside the layers is usually much lower than that at the interface. As a result, in our case even though there is no defect-related emission in PL, defect-related EL emission has been observed. This is the first report on MgZnO heterostructured LEDs and the shortest EL emission ever reported in ZnO-based p-n junction LEDs to the best of our knowledge.

To understand the origin of the 355 nm emission better, the band diagram of the p-$Mg_{0.35}Zn_{0.65}O$:(Li, N)/n-$Mg_{0.20}Zn_{0.80}O$ heterostructured LED under forward bias has been plotted, as shown in Fig. 5. Considering that the bandgap difference between $Mg_{0.35}Zn_{0.65}O$ and $Mg_{0.20}Zn_{0.80}O$ is 0.15 eV, and the ratio between the conduction band offset and valence band offset (ΔEc/ΔEv) in MgZnO is approximately 9:1 [22], the conduction band offset and valence band offset at the interface can be derived to be around 0.135 and 0.015 eV, respectively. Under forward bias, the conduction band offset will act as a barrier that hinders the drift of electrons from the n-$Mg_{0.20}Zn_{0.80}O$ layer to the p-$Mg_{0.35}Zn_{0.65}O$:(Li, N) layer; thus electrons will be confined in the n-$Mg_{0.20}Zn_{0.80}O$ layer. As for holes in the p-$Mg_{0.35}Zn_{0.65}O$:(Li, N) layer, they will be drifted into the n-$Mg_{0.20}Zn_{0.80}O$ layer under the drive of the bias voltage; then radiative recombination will occur in the n-$Mg_{0.20}Zn_{0.80}O$ layer. As a result, emission from the $Mg_{0.20}Zn_{0.80}O$ layer has been detected from the p-$Mg_{0.35}Zn_{0.65}O$:(Li, N)/n-$Mg_{0.20}Zn_{0.80}O$ heterostructured LED.

In conclusion, MgZnO-based heterostructured LEDs have been realized from a p-$Mg_{0.35}Zn_{0.65}O$:(Li, N)/n-$Mg_{0.20}Zn_{0.80}O$ structure. Obvious emission peaked at around 355 nm has been observed from the heterostructure, which can be attributed to the near-band-edge emission of the n-type $Mg_{0.20}Zn_{0.80}O$ layer. This is the first report on MgZnO heterostructured LEDs and the shortest EL emission ever reported in ZnO-based p-n junction LEDs to the best of our knowledge. The results reported in this paper may promise short UV or even deep ultraviolet LEDs from MgZnO-based materials.

This work is supported by the National Basic Research Program of China (2011CB302005), the Natural Science Foundation of China (11074248, 11104265, and 61177040), and the Science and Technology Developing Project of Jilin Province (20111801).

References

1. A. Sandhu, Nat. Photonics **1**, 38 (2007).
2. G. Lozano, D. J. Louwers, S. R. K. Rodriguez, S. Murai, O. T. A. Jansen, M. A. Verschuuren, and J. G. Rivas, Light Sci. Appl. **2**, e66 (2013).
3. D. C. Look, Mater. Sci. Eng. B **80**, 383 (2001).
4. U. Ozgur, Y. I. Alivov, C. Liu, A. Teke, M. A. Reshchikov, S. Dogan, V. Avrutin, S. J. Cho, and H. Morkoc, J. Appl. Phys. **98**, 041301 (2005).
5. Y. Chen, D. M. Bagnall, H. Koh, K. Park, K. Hiraga, Z. Zhu, and T. Yao, J. Appl. Phys. **84**, 3912 (1998).
6. A. Tsukazaki, T. Onuma, M. Ohtani, T. Makino, M. Sumiya, K. Ohtani, S. F. Chichibu, S. Fuke, Y. Segawa, H. Ohno, H. Koinuma, and M. Kawasaki, Nat. Mater. **4**, 42 (2005).
7. S. J. Jiao, Z. Z. Zhang, Y. M. Lu, D. Z. Shen, B. Yao, J. Y. Zhang, B. H. Li, D. X. Zhao, X. W. Fan, and Z. K. Tang, Appl. Phys. Lett. **88**, 031911 (2006).
8. Z. P. Wei, Y. M. Lu, D. Z. Shen, Z. Z. Zhang, B. Yao, B. H. Li, J. Y. Zhang, D. X. Zhao, X. W. Fan, and Z. K. Tang, Appl. Phys. Lett. **90**, 042113 (2007).
9. J. Dai, C. X. Xu, and X. W. Sun, Adv. Mater. **23**, 4115 (2011).
10. C. Yuen, S. F. Yu, S. P. Lau, Rusli, and T. P. Chen, Appl. Phys. Lett. **86**, 241111 (2005).
11. K. Nakahara, S. Akasaka, H. Yuji, K. Tamura, T. Fujii, Y. Nishimoto, D. Takamizu, A. Sasaki, T. Tanabe, H. Takasu, H. Amaike, T. Onuma, S. F. Chichibu, A. Tsukazaki, A. Ohtomo, and M. Kawasaki, Appl. Phys. Lett. **97**, 013501 (2010).
12. H. Kato, T. Yamamuro, A. Ogawa, C. Kyotani, and M. Sano, Appl. Phys. Express **4**, 091105 (2011).
13. L. Li, Z. Yang, J. Y. Kong, and J. L. Liu, Appl. Phys. Lett. **95**, 232117 (2009).
14. A. Ohtomo, M. Kawasaki, T. Koida, K. Masubuchi, H. Koinuma, Y. Sakurai, Y. Yoshida, T. Yasuda, and Y. Segawa, Appl. Phys. Lett. **72**, 2466 (1998).
15. H. Zhu, C. X. Shan, B. H. Li, J. Y. Zhang, B. Yao, Z. Z. Zhang, D. X. Zhao, D. Z. Shen, and X. W. Fan, J. Phys. Chem. C **113**, 2980 (2009).
16. H. Zhu, C. X. Shan, B. H. Li, Z. Z. Zhang, B. Yao, and D. Z. Shen, Appl. Phys. Lett. **99**, 101110 (2011).
17. F. Sun, C. X. Shan, B. H. Li, Z. Z. Zhang, D. Z. Shen, Z. Y. Zhang, and D. Fan, Opt. Lett. **36**, 499 (2011).
18. J. S. Liu, C. X. Shan, H. Shen, B. H. Li, Z. Z. Zhang, L. Liu, L. G. Zhang, and D. Z. Shen, Appl. Phys. Lett. **101**, 011106 (2012).
19. J. S. Liu, C. X. Shan, S. P. Wang, B. H. Li, Z. Z. Zhang, and D. Z. Shen, J. Cryst. Growth, **347**, 95 (2012).
20. B. Y. Zhang, B. Yao, Y. F. Li, Z. Z. Zhang, B. H. Li, C. X. Shan, D. X. Zhao, and D. Z. Shen, Appl. Phys. Lett. **97**, 222101 (2010).
21. S. H. Jeong, B. S. Kim, and B. T. Lee, Appl. Phys. Lett. **82**, 2625 (2003).
22. A. Ohtomo, M. Kawasaki, I. Ohkubo, H. Koinuma, T. Yasuda, and Y. Segawa, Appl. Phys. Lett. **75**, 980 (1999).